Pre-Clinical Research Report

Journal of INTERNATIONAL MEDICAL RESEARCH

Journal of International Medical Research
48(4) 1–14

DOI: 10.1177/0300060520903652
journals.sagepub.com/home/imr
SAGE

Titanium dioxide nanoparticles induce endoplasmic reticulum stress-mediated apoptotic cell death in liver cancer cells

Zhiwang Li[1,2,3], Jingliang He[4], Bowei Li[1], Jinqian Zhang[5], Ke He[2], Xiaopeng Duan[2], Rui Huang[2], Zuguang Wu[3] and Guoan Xiang[1,2]

Abstract

Objective: Titanium oxide (TiO_2) acts as a photosensitizer in photodynamic therapy by mediating reactive oxygen species (ROS)-induced endoplasmic reticulum (ER) stress. This study aimed to investigate the effect of TiO_2 on ER stress in liver cancer cells.

Methods: Normal human liver and human hepatocarcinoma cell lines were incubated with various concentrations of TiO_2 nanotubes for 48 hours. Cell growth, apoptosis, cell cycle, and cellular ROS were detected. Expression levels of ER stress sensors (PERK and ATF6) and Bax were evaluated by western blot. The effect of TiO_2 on liver cancer growth was also investigated in mice *in vivo*.

Results: TiO_2 inhibited cell growth, increased apoptosis and cellular ROS levels, and arrested the cell cycle in G1 stage in liver cancer cells. TiO_2 also increased PERK, ATF6, and Bax expression levels in liver cancer cells in dose-dependent manners. TiO_2 had no significant effect on cell growth, apoptosis, ROS level, cell cycle distribution, or PERK, ATF6, or Bax expression in normal liver cells. TiO_2 administration reduced tumor volume and increased PERK, Bax, and ATF6 expression levels in tumor tissues *in vivo*.

Conclusions: TiO_2 nanoparticles increased ROS-induced ER stress and activated the PERK/ATF6/Bax axis in liver cancer cells *in vitro* and *in vivo*.

[1]Department of General Surgery, Guangdong Second Provincial General Hospital, Guangzhou, China
[2]The Second School of Clinical Medicine, Southern Medical University, Guangzhou, China
[3]Department of Gastrointestinal Surgery, Meizhou People's Hospital, Meizhou, China
[4]Shunde Hospital of Guangzhou University of Traditional Chinese Medicine, Foshan, China
[5]Department of Laboratory Medicine, Guangdong Second Provincial General Hospital, Guangzhou, China

Corresponding author:
Guoan Xiang, Department of General Surgery, Guangdong Second Provincial General Hospital, The Second School of Clinical Medicine, Southern Medical University, Guangzhou, Guangdong 510317, P.R. China.
Email: guoan_66@163.com

Keywords
Titanium dioxide, nanoparticles, hepatocellular carcinoma, nanotoxicity, endoplasmic reticulum stress, apoptosis

Date received: 22 June 2019; accepted: 8 January 2020

Introduction

Liver cancer is one of the most common malignancies and a leading cause of cancer-related death worldwide.[1] Numerous studies have demonstrated that some pharmaceutical agents can induce liver cancer cell apoptosis by triggering reactive oxygen species (ROS)-mediated endoplasmic reticulum (ER) stress.[2–4] However, liver cancer cell heterogeneity and drug resistance pose major obstacles to the treatment of liver cancer. Recent evidence has indicated that nanoparticles conjugated with pharmaceutical agents or genetic vectors can enhance drug sensitivity in cancer cells.[5–7]

Nanoscaled titanium oxide (TiO_2) photocatalyst has been regarded as a potential photosensitizer in ultraviolet light-driven photodynamic therapy, and has been widely used in clinical cancer treatments based on its photocatalytic, biocompatible, and favorable mechanical properties.[8–10] Photoexcited TiO_2 affects cellular functions by driving ROS production and thus exerting nanotoxicity in cancer cells.[11] TiO_2 particles can induce malignant cell apoptotic death via the production of ROS,[12] and ROS on the surface of TiO_2 nanoparticles caused oxidative stress in adjacent cells or tissues, and preferentially damaged cancer cells.[12,13] However, information about the therapeutic effect of TiO_2 in liver cancer and its underlying mechanisms is still lacking.

ROS-induced accumulation of misfolded and unfolded polypeptides in the ER activates the adaptive intracellular stress response (unfolded protein response) to reduce ER stress by correcting or degrading misfolded polypeptides within the ER.[14,15] The ROS-induced ER stress response can trigger cell apoptosis by inducing the expression of ER sensor proteins, including protein kinase RNA-like endoplasmic reticulum kinase (PERK), activating transcription factor 6 (ATF6), eukaryotic initiation factor (eIF) 1, and X-box binding protein 1, and their downstream signaling pathways, such as the PERK/eIF2α/ATF4/CCAAT enhancer-binding protein homologous protein (CHOP) pathway.[16,17] The ER stress response and the induction of these genes or pathways have been identified in many diseases such as oxidative-stressed liver,[18] breast cancer,[12] liver cancer,[19] and glioma cells.[20] Nanoparticle-induced ER stress is an early biomarker for nanotoxicity evaluation.[21] Moreover, ER stress-mediated cancer cell apoptosis has been reported to be involved in the cytotoxic effect of TiO_2.

In this study, we investigated the toxicity and underlying mechanism of TiO_2 in liver cancer cells to reveal its potential therapeutic application in patients with liver cancer.

Materials and methods

Cell lines and culture conditions

The human normal liver cell line L02 and human hepatocarcinoma cell line HepG2 were obtained from the American Type Culture Collection (Manassas, VA, USA). Cells were revivified and cultured in

Dulbecco's Modified Eagle Medium (DMEM; Gibco, Burlington, ON, Canada) supplemented with 10% fetal bovine serum (Gibco) in a humidified 5% CO_2 incubator at 37°C.

Cellular TiO_2 treatment

TiO_2 nanoparticles were purchased from ACMEC Biochemical Co., Ltd. (Shanghai, China; cat. no. T446775-1g). Experimental TiO_2 nanoparticles were stored in our laboratory, and TiO_2 nanoparticles solution (50 μg/mL) was prepared in 75% ethanol. Solutions of TiO_2 nanoparticles (400 μL) at concentrations of 0, 2.5, 5.0, 7.5, and 10 μg/mL in 75% ethanol were added to the bottom layer of 6-well plates (Costar Corning Inc., Corning, NY, USA) and incubated in an electric thermostatically controlled incubator at 60°C (DHP-9162, Shanghai Yiheng Technical Co., Ltd., Shanghai, China). Prior to cell treatment, dry plates were sterilized with ultraviolet light on a clean bench for 2 hours. For TiO_2 treatment, 2 mL of cell cultures (density 1×10^5 cells/mL) were added into the 6-well plates coated with TiO_2 and maintained for 48 hours. Each experiment was performed in triplicate.

Cell counting analysis

Cells in logarithmic growth were treated with TiO_2 for 48 hours, harvested, centrifuged at $151 \times g$ for 5 minutes, and diluted with 2 mL DMEM (Gibco). The cells were then placed in plates and cell numbers were counted under an inverted microscope (×100, Axiovert 40C; Carl Zeiss, OberkochenWuertt, Germany). Cell number was calculated as the average cell number from four chambers $\times 10^4$.

Cell cycle and Annexin V apoptosis assay

Cells were harvested from the 6-well plates using trypsin, after TiO_2 treatment for 48 hours (Gibco). For cell cycle analysis, cells were harvested and labeled with propidium iodide (PI), followed by flow cytometry analysis (Becton Dickinson Immunocytometry Systems, San Jose, CA, USA). For cell apoptosis analysis, cells were washed with 1× phosphate-buffered saline (PBS) (pH 7.2), resuspended in $1 \times$ Annexin V-binding buffer (BioLegend, San Diego, CA, USA), centrifuged at $97 \times g$ for 3 minutes, and then resuspended in 100 μL $1 \times$ Annexin V-binding buffer. Apoptotic cells and necrosis were detected by flow cytometry (Becton Dickinson Immunocytometry Systems) after staining with Annexin V-fluorescein isothiocyanate and 7-aminoactinomycin D (BioLegend).

Measurement of ROS

Cellular ROS levels were measured by 2′, 7′-dichlorofluorescin diacetate (DCFDA) flow cytometric analysis. After treatment with TiO_2 nanoparticles, the cells were incubated with 10 μM DCFDA staining solution (Beyotime Biotech, Nantong, China) at 37°C and 5% CO_2 for 20 minutes. Cellular ROS levels were then measured using a BD flow cytometer (BD Biosciences, San Jose, CA, USA).

Animal model

The animal experiment protocols were approved by the Ethics Committee of Guangdong Second Provincial General Hospital. Male BALB/C nude mice (weight 15–20 g; Laboratory Animal Center of Southern Medical University, Guangzhou, China) were allowed to acclimatize for 5 days under specific-pathogen-free conditions with free access to food and water. A subcutaneous tumor model was created by injection of 4×10^6 HepG2 cells per mouse. Fourteen days later, 30 tumor-bearing mice were divided randomly into two groups ($n = 15$ per group) and treated

by intratumoral injection of 200 μL (nano sol in distilled water) of PBS (control group) or 1 mg/mL TiO_2 nanomaterials. TiO_2 administration was performed every 6 days. All mice were sacrificed 30 days later by intraperitoneal injection of a lethal dose of sodium pentobarbital. Death was confirmed by cessation of breathing and heartbeat. Tumor tissues were separated and tumor volume was measured. The samples were then fixed or frozen in liquid nitrogen for immunohistochemical and western blot analysis, respectively.

Immunohistochemistry

Fixed tumor tissues were transparentized, embedded in paraffin, and cut into 4-μm sections. Endogenous peroxidase activity was quenched and the sections were blocked with normal goat serum (Gibco) for 30 minutes. The sections were then incubated with specific primary monoclonal antibodies against ATF6 (dilution 1:250; Abcam, Cambridge, MA, USA) and phospho-PERK (dilution 1:200; Abcam) for 12 hours at 4°C, followed by incubation with horseradish peroxidase (HRP)-labeled goat anti-rabbit/rat IgG secondary antibody (dilution 1:1000, Santa Cruz Biotechnology, Santa Cruz, CA, USA) at room temperature for 4 hours. ATF6- and PERK-positive cells were visualized using diaminobenzidine staining and images were obtained using an Olympus microscope (BX51T-PHD-J11, ×400, Olympus Corporation, Tokyo, Japan) after counterstaining with hematoxylin. Isotype-matched IgG antibody was used as a negative control.

Western blot analysis

Total protein was isolated from the cells and tumor samples. Tumor tissues were minced, ground, and homogenized in ice-cold RIPA lysis buffer (Fermentas, Thermo Fisher Scientific, Waltham, MA, USA) containing phenylmethylsulfonyl fluoride (PMSF; 100:1). Cells were harvested using trypsin (Gibco) and subjected to ice-cold RIPA lysis buffer (Fermentas, Thermo Fisher Scientific) containing PMSF (100:1). Lysates were centrifuged at 10800 × g for 15 minutes at 4°C, followed by quantification using a Pierce BCA protein assay kit (cat. no. 23225; Thermo Fisher Scientific). Equal amounts of protein (100 μg per sample) were separated by 10% sodium dodecyl sulfate-polyacrylamide gel electrophoresis (CWBIO, Beijing, China) and transferred onto polyvinylidene difluoride membranes (Millipore Filter Corp., Watertown, MA, USA) at 16 W for 30 minutes. Proteins on the membranes were subjected to immunoblotting according to standard procedures, using primary antibodies against ATF6 (dilution 1:1000; Abcam), phospho-PERK (dilution 1:1000; Abcam), anti-Bcl-2 family protein (Bax, dilution 1:1500), glyceraldehyde 3-phosphate dehydrogenase (dilution 1:2000; Abcam), and goat anti-rabbit/rat IgG (dilution 1:5000; Santa Cruz). Secondary HRP-labeled goat anti-rabbit/rat IgG antibody (dilution 1:5000; Santa Cruz) was then added and the membranes were developed by enhanced chemiluminescence (Millipore Corp., Watertown, MA, USA). The band pattern was visualized and imaged using a WD-9413B gel imaging analyzer (Beijing Liuyi Instrument Factory, Beijing, China).

All statistical analyses were carried out using SPSS 17.0 (IBM, Armonk, NY, USA). All data were expressed as mean ± standard deviation of triplicate experiments or five samples. For multiple comparisons, normally distributed data sets with equal variances (Bartlett's test) were analyzed by one-way analysis of variance (ANOVA) with *post hoc* Student–Newman–Keuls tests. Non-normally distributed data were analyzed using non-parametric Kruskal–Wallis followed by Dunn's multiple

comparison tests. $P < 0.05$ was considered statistically significant. Graphs were constructed using GraphPad Prism 6.0 (GraphPad Software Inc. La Jolla, CA, USA).

Results

TiO_2 inhibited liver cancer cell growth

The effect of TiO_2 on the growth of liver cancer cells was determined by cell counting analysis, using normal hepatic epithelial L02 cells as a control. TiO_2 had no significant effect on the growth of L02 cells (Figure 1a). In contrast, plate-coated TiO_2 nanotubes significantly inhibited the proliferation of liver cancer cells at concentrations of 5.0, 7.5, and 10 μg/mL ($P < 0.05$ or <0.01) (Figure 1b), suggesting that TiO_2 inhibited liver cancer cell growth in a dose-dependent manner.

TiO_2 promoted the apoptosis of liver cancer cells by cell cycle arrest at G1 stage

Flow cytometry analysis showed not obvious effect of TiO_2 on the apoptosis of L02 cells (Figure 2a). In contrast, plate-coated TiO_2 significantly increased the percentage of apoptotic liver cancer cells in a dose-dependent manner ($P < 0.05$) (Figure 2b). TiO_2 thus promoted the apoptosis of liver cancer cells but had little effect on normal liver cells. Regarding cell cycle analysis, TiO_2 treatment had no significant effect on cell cycle progression in L02 cells (Figure 3a), but significantly increased the percentage of G1 stage and decreased the percentage of S phase HepG2 cells ($P < 0.05$) (Figure 3b). These results revealed that TiO_2 promoted the apoptosis of liver cancer cells by blocking the cell cycle in G1 phase.

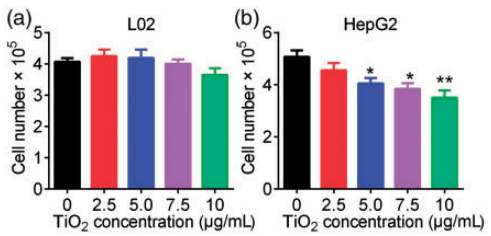

Figure 1. Influence of TiO_2 nanotubes on cell growth. L02 (a) and HepG2 (b) cells were incubated in TiO_2 nanotube-coated (2.5, 5.0, 7.5, and 10 μg/mL) 6-well plates for 48 hours at 60°C. Cell numbers were counted using cell counting chambers. Cells incubated in 6-well plates coated with 0 μg/mL TiO_2 nanotubes were used as a control. *$P < 0.05$ and **$P < 0.01$ vs. 0 μg/mL (control).

TiO_2 increased ROS accumulation in liver cancer cells

We investigated the effect of TiO_2 on oxidative stress in liver cancer cells by measuring ROS levels by DCFDA flow cytometry. ROS levels in L02 cells were unaffected by TiO_2 treatment, but ROS levels in liver cancer cells were significantly increased by TiO_2 in a dose-dependent manner ($P < 0.001$) (Figure 4), indicating that TiO_2 treatment enhanced oxidative stress in liver cancer cells.

TiO_2 activated ER stress responses

ER stress-mediated apoptosis in cancer cells represents a pharmacological mechanism for cancer therapy.[22,23] We determined if TiO_2-mediated cell apoptosis in liver cancer cells was associated with ER stress by detecting the expression levels of the ER stress-related transducers/sensors ATF6 and PERK by western blotting. Expression levels of PERK and ATF6 in L02 cells were low and were unaffected by incubation with TiO_2 nanoparticles for 48 hours (Figure 5a). In contrast, expression levels of PERK and ATF6 were significantly increased ($P < 0.001$) in HepG2 liver cancer cells in line with increasing TiO_2 nanoparticle concentrations (Figure 5b).

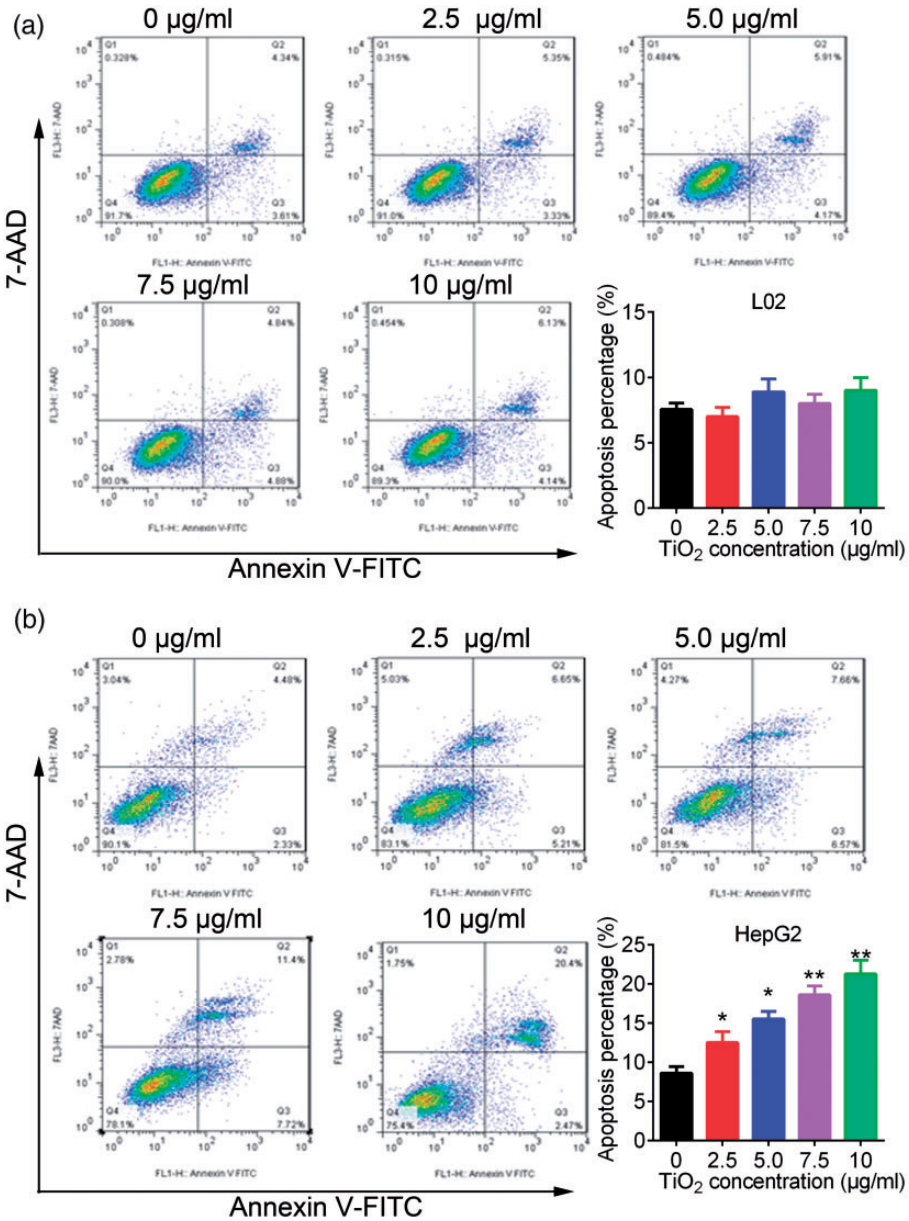

Figure 2. L02 (a) and HepG2 (b) cells were cultured in 6-well plates for 48 hours, then apoptosis of L02 cells and HepG2 cells was detected by flow cytometry. TiO_2 increased the percentage of apoptotic liver cancer cells. Annexin V-positive cells were considered as apoptotic liver cancer cells. Cells incubated with 0 μg/mL TiO_2 were used as a control. *$P < 0.05$ and **$P < 0.01$ vs. 0 μg/mL (control). AAD, 7-amino-actinomycin D.

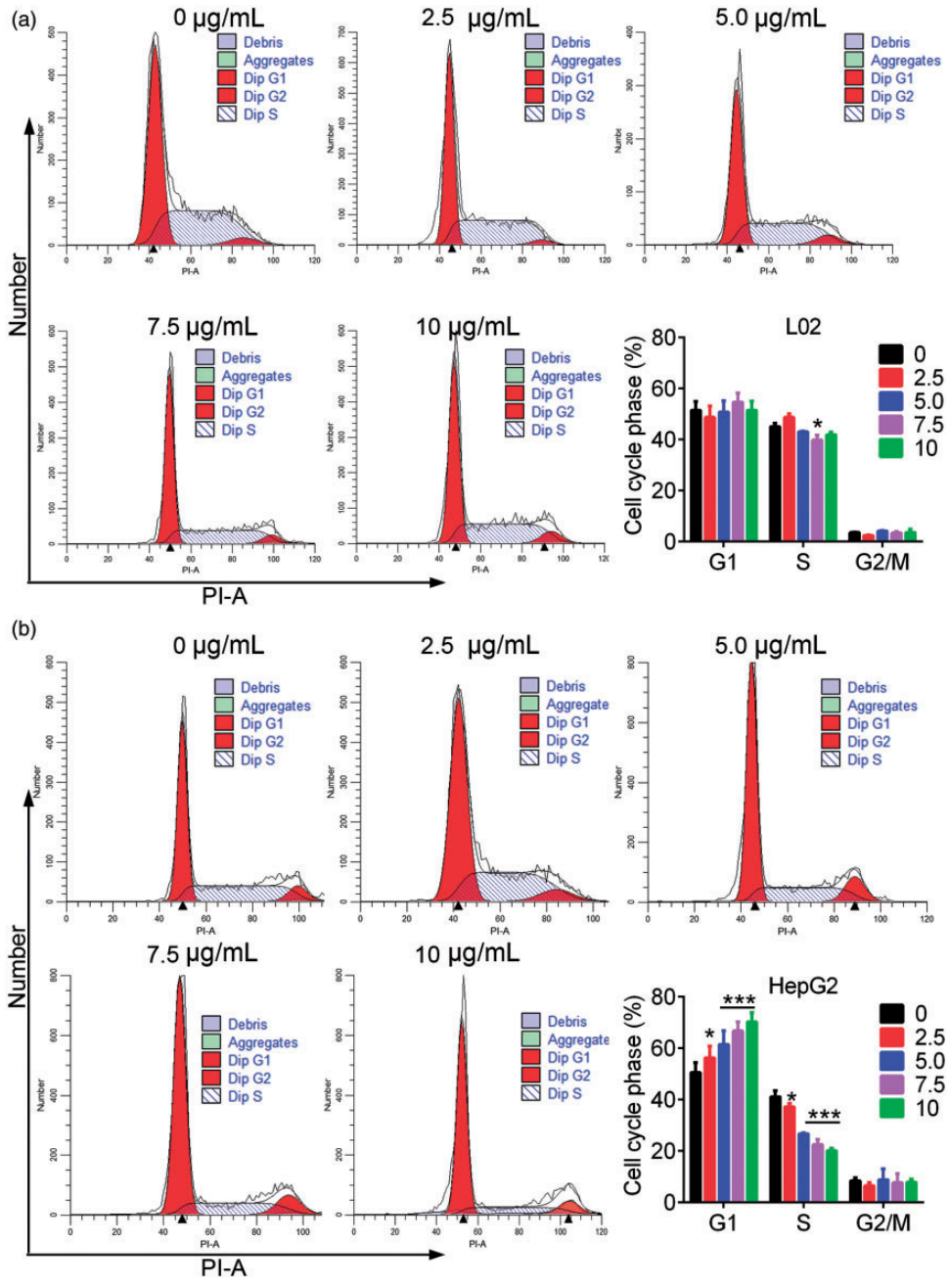

Figure 3. L02 (a) and HepG2 (b) cells were incubated in TiO_2 for 48 hours and analyzed by flow cytometry with propidium iodide. TiO_2 induced liver cancer cell cycle arrest in the G1 phase. Cells incubated with 0 μg/mL TiO_2 were used as a control. $^*P < 0.05$, $^{**}P < 0.01$, and $^{***}P < 0.001$ vs. 0 μg/mL (control). PI-A, propidium iodide area; Dip, diploid.

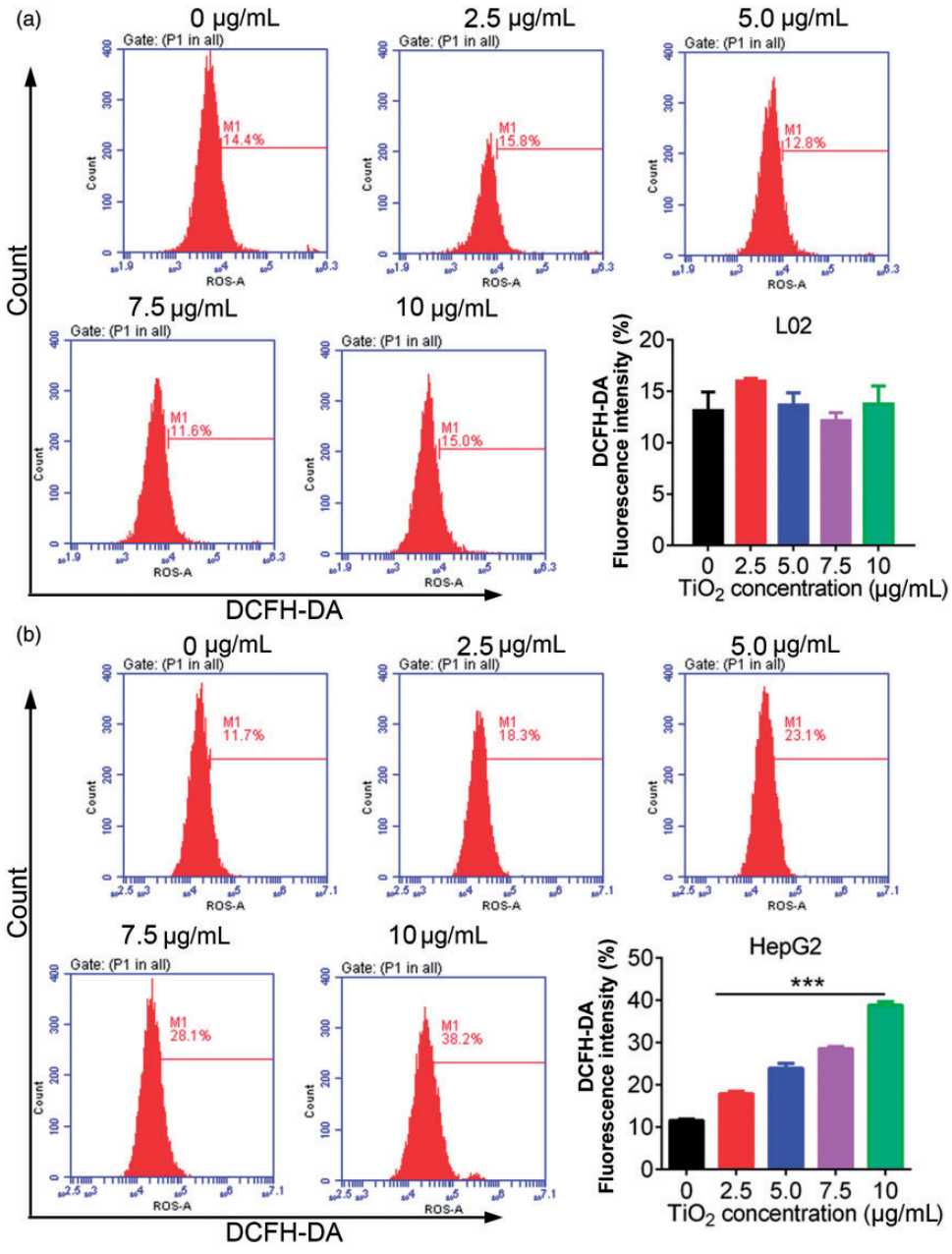

Figure 4. L02 (a) and HepG2 (b) cells were treated with 0, 2.5, 5.0, 7.5, and 10 μg/mL TiO_2, and the cell cycle distribution was then examined by flow cytometry. TiO_2 caused release of ROS in liver cancer cells. Cells incubated with 0 μg/mL TiO_2 were used as a control. ***$P < 0.001$ vs. 0 μg/mL (control). DCFDA, 2',7'-dichlorofluorescin diacetate.

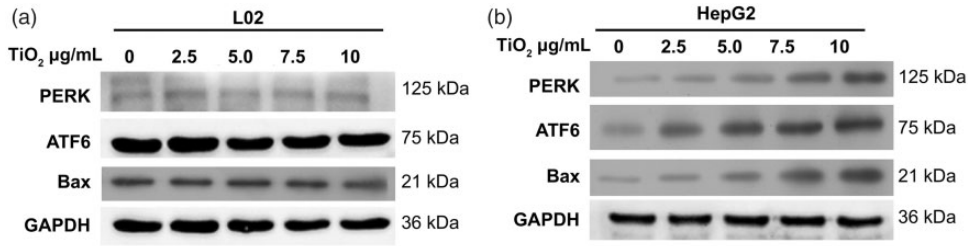

Figure 5. Western blot analysis of cellular proteins. L02 (a) and HepG2 (b) cells were treated with 0, 2.5, 5.0, 7.5, and 10 μg/mL TiO_2 nanotubes for 48 hours and ATF6 and PERK protein levels were then detected by western blot analysis. Cells treated with 0 μg/mL TiO_2 were used as a control and glyceraldehyde 3-phosphate dehydrogenase was used as an internal reference. PERK, protein kinase RNA-like endoplasmic reticulum kinase; ATF6, activating transcription factor 6; GAPDH, glyceraldehyde 3-phosphate dehydrogenase.

Bax protein expression levels were also increased by TiO_2 treatment in a dose-dependent manner in HepG2 cells, but not in L02 cells. These data suggested that TiO_2 nanoparticles activated the ER stress response in liver cancer cells but not in normal liver cells, and might thus contribute to the TiO_2-mediated apoptosis of liver cancer cells.

TiO_2 inhibited liver cancer tumorigenesis in vivo

Our *in vitro* experiments showed that TiO_2 inhibited the growth and promoted the apoptosis of liver cancer cells. We therefore speculated that TiO_2 might also inhibit the tumorigenesis or development of liver cancer *in vivo*. To verify this hypothesis, we inoculated nude BALB/C mice subcutaneously with HepG2 cells and treated them with or without TiO_2 nanoparticles for 30 days. Tumor volumes were significantly smaller in mice treated with TiO_2 nanoparticles (1 mg/mL) compared with control PBS-treated mice (5 weeks, $P = 0.045$; 6 weeks, $P = 0.037$; 7 weeks $P = 0.035$) (Figure 6a and 6b). Moreover, the percentages of PERK-, ATF6-, and Bax-positive cells in the tumor tissues were increased in mice treated with TiO_2 ($P = 0.031$) (Figure 6c). Protein expression levels of ATF6, Bax, and PERK were also upregulated in TiO_2-treated tumors according to western blot analysis ($P = 0.008$) (Figure 6d). These results confirmed that TiO_2 also inhibited tumor growth *in vivo* by activating ER stress and inducing cell apoptosis.

Discussion

The biocompatibility and favorable mechanical properties of TiO_2 have supported its wide clinical application.[8,9] Increasing evidence has shown that TiO_2-mediated toxicity induced apoptotic death in cancer cells.[9,12] In the current study, TiO_2 treatment increased apoptosis in liver cancer cells but not normal liver cells, suggesting the safety of TiO_2 treatment.

We carried out cell cycle analysis to clarify the mechanism by which TiO_2 promoted apoptosis. Cell cycle arrest is closely associated with cell growth retardation and apoptosis.[24] Tumor cells may only be sensitive to certain drugs at specific stages of the cell cycle, and modulating the cell cycle pharmacologically may thus increase the efficacy of regular chemotherapy. The cell cycle can be divided into G1, S, and G2/M phases. In the current study, TiO_2 treatment increased the percentage of G1 phase liver cancer cells

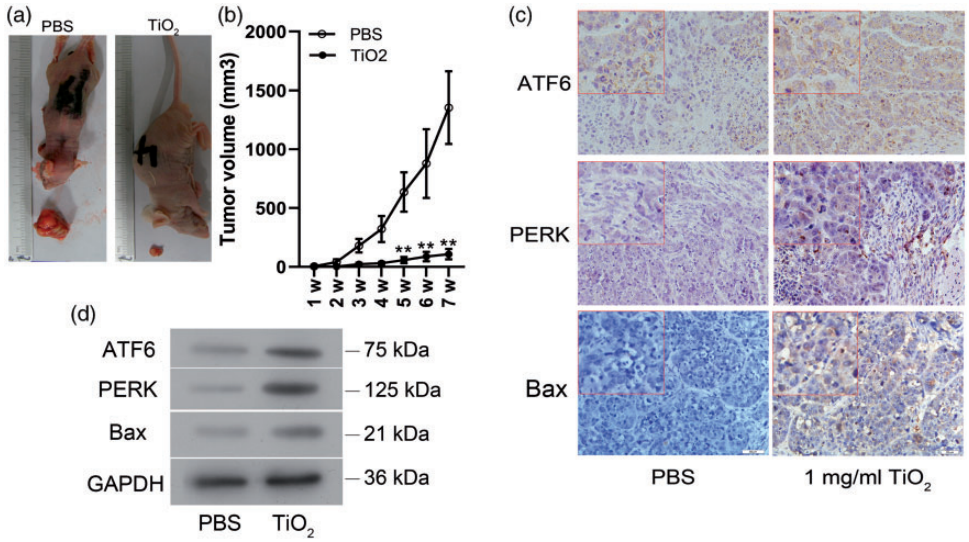

Figure 6. Effects of TiO_2 on tumors in BALB/C mice *in vivo*. (a) Liver cancer cells were injected subcutaneously into the right forelimbs of male BALB/C nude mice, followed by treatment with PBS or TiO_2 nanotubes. (b) Tumor volumes. ATF6, PERK, and Bax protein expression levels in tumor tissues detected by immunohistochemistry (×400) (c) and western blot analysis (d). Mice treated with PBS were used as a control. Magnification, ×40; magnification of the inserted red-lined boxes in the panels, ×400. PBS, phosphate-buffered saline; ATF6, activating transcription factor 6; PERK, protein kinase RNA-like endoplasmic reticulum kinase; GAPDH, glyceraldehyde 3-phosphate dehydrogenase; w, weeks.

and decreased the percentages of S and G2/M phase cells, suggesting that the synthesis of RNA and ribosomes were blocked, thus preventing the cells from entering the next stage of the cell cycle and leading to increased apoptosis.

Ultraviolet-A irradiation-stimulated photocytotoxicity of TiO_2 is mediated by the generation of ROS and oxidative stress in the target tissues or cells.[12,13] ER stress is associated with increasing ROS,[25] and prolonged high levels of ROS induce irreversible damage to proteins and lead to misfolded and unfolded polypeptides in the ER,[26] resulting in reduced production of ribosomes and RNA and G1 phase cell cycle arrest.[14] ER stress is characterized by the activation of several ER sensors, including PERK and ATF6.[27] In the present study, we demonstrated that PERK and ATF6 were upregulated and ROS levels were increased in TiO_2-treated liver cancer cells, suggesting that TiO_2 promoted ER stress-mediated apoptosis of liver cancer cells.

The ER sensors and their downstream signaling pathways play important roles in regulating cancer cell apoptosis.[28] ER stress can cause PERK and ATF6 to dissociate from GRP78, thus activating the PERK and ATF pathways.[29] Both PERK and ATF6 pathways can mediate CHOP expression and induce apoptosis.[30] Previous studies showed that the PERK/eIF2α/ATF4/CHOP signaling pathway played crucial roles in ROS–ER stress-induced apoptosis.[18,31,32] PERK/eIF2a signaling pathway-mediated apoptosis has also been reported in hypoxia-cultured cardiomyocytes,[32,33] smoke extract-cultured human bronchial epithelial cells,[34] and in hepatocytes from rats with alcoholic liver injury.[18]

Knockdown of CHOP decreased wogonin (V8)-mediated apoptosis and the activation of multiple ER stress markers in liver cancer cells.[19] ATF4 and GRP78 expression levels are mediated by cleavage of caspases 3, 7, and 12,[35,36] and ATF6 and GRP78 activation have been observed in hepatocellular carcinoma.[37] During ER stress-mediated apoptosis, ATF6 increased the production of CHOP and GRP78, ultimately leading to activation of the caspase cascade to execute ER stress-induced glioma cell apoptosis.[20] These findings demonstrated that PERK and ATF6 activation were critical for cancer cell apoptosis. Our data accordingly showed that TiO_2-induced ROS production was accompanied by increased Bax expression (as a Bcl-2 family apoptosis promoter), indicating the role of the PERK/ATF/Bax/caspase axis in TiO_2-induced apoptosis in liver cancer cells.

TiO_2 has been reported to increase the sensitivity of cancer cells (MCF-7 and MKN-45) to radiation by increasing ROS production.[38] Enhanced radiosensitivity of cancer cells by nanoparticles (nanocores) has also been reported *in vitro*.[39,40] The PERK/eIF2a pathway was shown to confer radioresistance in oropharyngeal and hepatocellular carcinoma by modulating the ER stress response.[41,42] Chen *et al.*[41] suggested that knockdown of GRP78 or ATF6 by small interfering RNA enhanced cisplatin-induced apoptosis. Furthermore, Qiao *et al.*[42] showed that overexpression of PERK was correlated with a poor prognosis in patients with oropharyngeal carcinoma, and that PERK silencing increased the radiosensitivity by increasing radiation-induced apoptosis in oropharyngeal carcinoma cells. Cancer cell radioresistance conferred by the PERK/eIF2a pathway might provide an interesting insight into TiO_2-mediated radiosensitivity and cancer cell apoptosis.

The present study confirmed that TiO_2 enhanced ER stress and increased apoptosis in liver cancer cells, but had no obvious effect in L02 cells. These differences might be due to the differential expression patterns of stress-response genes and the metabolic changes in cancer cells compared with normal cells.[43] TiO_2 had a significant toxic effect in human breast cancer SKBR3 cells but not in human embryonic kidney HEK293 cells.[44] However, high concentrations of TiO_2 nanoparticles were shown to induce serious cytotoxicity in some normal cells.[44,45] Kim *et al.*[45] showed that the IC_{50} value of TiO_2 nanoparticles in a normal cell line (L-132) was markedly higher than that in A549 lung cancer cells, demonstrating dose-dependent nanocytotoxicity between normal and cancer cells. This was in accordance with our current results, which showed obvious toxicity of TiO_2 in liver cancer cells but not in L02 cells. TiO_2 thus promoted cell growth inhibition and apoptosis in liver cancer cells both *in vitro* and *in vivo*. However, further experiments are needed to explore the mechanisms underlying TiO_2-mediated toxicity and radiosensitivity in liver cancer cells, and to determine the optimal concentrations of TiO_2 nanoparticles in liver cancer cells and tumor-bearing mice.

In conclusion, we demonstrated that TiO_2 could induce cytotoxicity in liver cancer cells, with no obvious adverse effects in normal liver cells. Mechanistically, TiO_2 increased ROS production and thus triggered the ER stress-related PERK/ATF6/Bax signaling pathway in liver cancer cells.

Declaration of conflicting interest

The authors declare that there is no conflict of interest.

Funding

This research received no specific grant from any funding agency in the public, commercial, or not-for-profit sectors.

ORCID iD

Zhiwang Li https://orcid.org/0000-0003-1623-8059

References

1. Yang F, Li QJ, Gong ZB, et al. MicroRNA-34a targets Bcl-2 and sensitizes human hepatocellular carcinoma cells to sorafenib treatment. *Technol Cancer Res Treat* 2014; 13: 77–86.
2. Sengupta D, Chatterjee S, Chatterjee T, et al. SAC and Berberine mediated repression of reactive species and hepatoprotection after DEN + CCl_4 exposure. *Proceedings of the Zoological Society* 2017; 70: 28–41.
3. Song T, Xu H, Sun N, et al. Metabolomic analysis of alfalfa (*Medicago sativa* L.) root-symbiotic rhizobia responses under alkali stress. *Front Plant Sci* 2017; 8: 1208.
4. Mortezaee K. Human hepatocellular carcinoma: protection by melatonin. *J Cell Physiol* 2018; 233: 6486–6508.
5. Rolfo C, Fanale D, Hong DS. Impact of MicroRNAs in resistance to chemotherapy and novel targeted agents in non-small cell lung cancer. *Curr Pharm Biotechnol* 2014; 15: 475–485.
6. Tan L, Li Y, Yang X, et al. Genetic diversity and drug sensitivity studies on *Eimeria tenella* field isolates from Hubei Province of China. *Parasit Vectors* 2017; 10: 137.
7. Ullah E, Mall R, Bensmail H, et al. Identification of cancer drug sensitivity biomarkers. *IEEE International Conference on Bioinformatics & Biomedicine*. 2017.
8. Tian A, Qin X, Wu A, et al. Nanoscale TiO2 nanotubes govern the biological behavior of human glioma and osteosarcoma cells. *Int J Nanomedicine* 2015; 10: 2423–2439.
9. Zhang S, Yang D, Jing D, et al. Enhanced photodynamic therapy of mixed phase TiO_2(B)/anatase nanofibers for killing of HeLa cells. *Nano Research* 2014; 7: 1659–1669.
10. Ahamed M, Khan MA, Akhtar MJ, et al. Role of Zn doping in oxidative stress mediated cytotoxicity of TiO_2 nanoparticles in human breast cancer MCF-7 cells. *Sci Rep* 2016; 6: 30196.
11. Ahamed M, Khan MAM, Akhtar MJ, et al. Ag-doping regulates the cytotoxicity of TiO_2 nanoparticles via oxidative stress in human cancer cells. *Sci Rep* 2017; 7: 17662.
12. Lagopati N, Tsilibary EP, Falaras P, et al. Effect of nanostructured TiO_2 crystal phase on photoinduced apoptosis of breast cancer epithelial cells. *Int J Nanomedicine* 2014; 9: 3219–3230.
13. Imani R, Dillert R, Bahnemann DW, et al. Multifunctional gadolinium-doped mesoporous TiO_2 nanobeads: photoluminescence, enhanced spin relaxation, and reactive oxygen species photogeneration, beneficial for cancer diagnosis and treatment. *Small* 2017; 13: 1700349. DOI: 10.1002/smll.201700349.
14. Zhang K, Wang S, Malhotra J, et al. The unfolded protein response transducer IRE1α prevents ER stress-induced hepatic steatosis. *EMBO J* 2011; 30: 1357–1375.
15. Kritsiligkou P, Rand JD, Weids AJ, et al. ER stress-induced reactive oxygen species (ROS) are detrimental for the fitness of a thioredoxin reductase mutant. *J Biol Chem* 2018; 293: 11984–11995.
16. Chalmers F, van Lith M, Sweeney B, et al. Inhibition of IRE1α-mediated XBP1 mRNA cleavage by XBP1 reveals a novel regulatory process during the unfolded protein response. *Wellcome Open Res* 2017. 2: 36.
17. Liu D, Zhou Y, Peng Y, et al. Endoplasmic reticulum stress in spinal cord contributes to the development of morphine tolerance. *Front Mol Neurosci* 2018; 11: 72.
18. Han XH, Wang JY, Wang L, et al. Role of PERK/eIF2a signaling pathway in hepatocyte apoptosis of alcoholic liver injury rats. *Chinese Journal of Hepatology* 2010; 18: 768–772.
19. Zhang Y, Zhao L, Li X, et al. V8, a newly synthetic flavonoid, induces apoptosis through ROS-mediated ER stress pathway in hepatocellular carcinoma. *Arch Toxicol* 2014; 88: 97–107.
20. Shen S, Zhang Y, Wang Z, et al. Bufalin induces the interplay between apoptosis and autophagy in glioma cells through endoplasmic reticulum stress. *Int J Biol Sci* 2014; 10: 212–224.

21. Chen R, Huo L, Shi X, et al. Endoplasmic reticulum stress induced by zinc oxide nanoparticles is an earlier biomarker for nanotoxicological evaluation. *ACS Nano* 2014; 8: 2562–2574.
22. Park IJ, Kim MJ, Park OJ, et al. Cryptotanshinone induces ER stress-mediated apoptosis in HepG2 and MCF7 cells. *Apoptosis* 2012; 17: 248–257.
23. Du S, Zhou J, Jia Y, et al. SelK is a novel ER stress-regulated protein and protects HepG2 cells from ER stress agent-induced apoptosis. *Arch Biochem Biophys* 2010; 502: 137–143.
24. Lagunes I, Martín-Batista E, Silveira-Dorta G, et al. Differential mechanism of action of the CK1ε inhibitor GSD0054. *J Mol Clin Med* 2018; 1: 77–84.
25. Sato AY, Tu X, McAndrews KA, et al. Prevention of glucocorticoid induced-apoptosis of osteoblasts and osteocytes by protecting against endoplasmic reticulum (ER) stress in vitro and in vivo in female mice. *Bone* 2015; 73: 60–68.
26. Papa L and Germain D. SirT3 regulates the mitochondrial unfolded protein response. *Mol Cell Biol* 2014; 34: 699–710.
27. Lerner AG, Upton JP, Praveen PV, et al. IRE1α induces thioredoxin-interacting protein to activate the NLRP3 inflammasome and promote programmed cell death under irremediable ER stress. *Cell Metab* 2012; 16: 250–264.
28. Shi K, Wang D, Cao X, et al. Endoplasmic reticulum stress signaling is involved in mitomycin C (MMC)-induced apoptosis in human fibroblasts via PERK pathway. *PLoS One* 2013; 8: e59330.
29. Yin L, Dai Y, Cui Z, et al. The regulation of cellular apoptosis by the ROS-triggered PERK/EIF2α/chop pathway plays a vital role in bisphenol A-induced male reproductive toxicity. *Toxicol Appl Pharmacol* 2017; 314: 98–108.
30. Fernández A, Ordóñez R, Reiter RJ, et al. Melatonin and endoplasmic reticulum stress: relation to autophagy and apoptosis. *J Pineal Res* 2015; 59: 292–307.
31. Liu ZW, Zhu HT, Chen KL, et al. Protein kinase RNA- like endoplasmic reticulum kinase (PERK) signaling pathway plays a major role in reactive oxygen species (ROS)-mediated endoplasmic reticulum stress- induced apoptosis in diabetic cardiomyopathy. *Cardiovasc Diabetol* 2013; 12: 158.
32. He Y, et al. PERK-eIF2 alpha signaling pathway involved in hypoxia-induced apoptosis in cultured cardiomyocytes. *Cardiovascular Therapeutics* 2012; 30(Suppl 1): 39–40.
33. Liu CL, Li X, Hu GL, et al. Salubrinal protects against tunicamycin and hypoxia induced cardiomyocyte apoptosis via the PERK-eIF2α signaling pathway. *J Geriatr Cardiol* 2012; 9: 258–268.
34. Yuan T, Luo BL, Wei TH, et al. Salubrinal protects against cigarette smoke extract-induced HBEpC apoptosis likely via regulating the activity of PERK-eIF2α signaling pathway. *Arch Med Res* 2012; 43: 522–529.
35. Martin S, Lamb HK, Brady C, et al. Inducing apoptosis of cancer cells using small-molecule plant compounds that bind to GRP78. *Br J Cancer* 2013; 109: 433–443.
36. de la Cadena SG, Hernández-Fonseca K, Camacho-Arroyo I, et al. Glucose deprivation induces reticulum stress by the PERK pathway and caspase-7- and calpain-mediated caspase-12 activation. *Apoptosis* 2014; 19: 414–427.
37. Shuda M, Kondoh N, Imazeki N, et al. Activation of the ATF6, XBP1 and grp78 genes in human hepatocellular carcinoma: a possible involvement of the ER stress pathway in hepatocarcinogenesis. *J Hepatol* 2003; 38: 605–614.
38. Rezaei-Tavirani M, Dolat E, Hasanzadeh H, et al. TiO_2 nanoparticle as a sensitizer drug in radiotherapy: in vitro study. *Iranian Journal of Cancer Prevention* 2013; 6: 37–44.
39. Fang X, Wang Y, Ma X, et al. Mitochondria-targeting Au nanoclusters enhance radiosensitivity of cancer cells. *J Mater Chem B* 2017; 5: 4190–4197. doi: 10.1039/C7TB00422B
40. Ma J, Xu R, Sun J, et al. Nanoparticle surface and nanocore properties determine the effect on radiosensitivity of cancer cells upon ionizing radiation treatment. *J Nanosci Nanotechnol* 2013; 13: 1472–1475.

41. Chen R, Dai RY, Duan CY, et al. Unfolded protein response suppresses cisplatin-induced apoptosis via autophagy regulation in human hepatocellular carcinoma cells. *Folia Biol (Praha)* 2011; 57: 87–95.
42. Qiao Q, Sun C, Han C, et al. Endoplasmic reticulum stress pathway PERK-eIF2α confers radioresistance in oropharyngeal carcinoma by activating NF-κB. *Cancer Sci* 2017; 108: 1421–1431.
43. Cui J, Chen J, Chen S, et al. Au/TiO_2 nano-belt heterostructures for the detection of cancer cells and anticancer drug activity by potential sensing. *Nanotechnology* 2016; 27: 095603.
44. Tahermansouri H, Islami F, Gardaneh M, et al. Functionalisation of multiwalled carbon nanotubes with thiazole derivative and their influence on SKBR3 and HEK293 cell lines. *Materials Technology* 2016; 31: 371–376. doi: 10.1179/1753555715Y.0000000062.
45. Kim IS, Baek M and Choi SJ. Comparative cytotoxicity of Al_2O_3, CeO_2, TiO_2 and ZnO nanoparticles to human lung cells. *J Nanosci Nanotechnol* 2010; 10: 3453–3458.